

Article

Understanding the PLA–Wood Adhesion Interface for the Development of PLA-Bonded Softwood Laminates

Warren J. Grigsby , Marc Gaugler  and Desiree Torayno

Manufacturing and Bioproducts, Scion, Rotorua 3010, New Zealand; marc.gaugler@scionresearch.com (M.G.); dmptorayno@gmail.com (D.T.)

* Correspondence: warrengrigsby1@gmail.com

Abstract: With polylactic acid (PLA) usage projected to increase in wood-based composite materials, a study comparing composite processing parameters with resulting PLA–wood adhesion and panel performance is warranted. In this study, PLA–softwood veneer laminates have been prepared and spatial chemical imaging via FTIR analysis was applied to identify PLA bondlines characterizing bondline thickness and the extent of PLA migration into the wood matrix. These PLA–wood adhesion interface characteristics have been compared with the performance of panels varying in pressing temperature, pressing time and PLA grades. For amorphous PLA, bondline thicknesses (60–120 μm) were similar, pressing at 140 $^{\circ}\text{C}$ or 160 $^{\circ}\text{C}$, whereas with semi-crystalline PLA, the bondline thickness (340 μm) significantly reduced (155–240 μm) only when internal panel temperatures exceeded 140 $^{\circ}\text{C}$ during pressing. Internal temperatures also impacted PLA penetration, with greater PLA migration from bondlines evident with higher pressing temperatures and times with distinctions between PLA grades and bondline position. Performance testing revealed thinner PLA bondlines were associated with greater dry strength for both PLA grades. Cold-water soaking revealed laminated panels exhibit a range of wet-strength performance related to panel-pressing regimes with the semi-crystalline PLA pressed at 180 $^{\circ}\text{C}$ having similar tensile strength in dry and wet states. Moreover, an excellent correlation between wet-strength performance and bondline thickness and penetration values was evident for this PLA grade. Overall, study findings demonstrate PLA wood composite performance can be tuned through a combination of the PLA grade and the pressing regime employed.

Keywords: poly(lactic acid); PLA; PLA bondlines; wood adhesives; plywood; wood veneer laminates; wood plastic composites; wood-adhesion interface



Citation: Grigsby, W.J.; Gaugler, M.; Torayno, D. Understanding the PLA–Wood Adhesion Interface for the Development of PLA-Bonded Softwood Laminates. *Fibers* **2022**, *10*, 51. <https://doi.org/10.3390/fib10060051>

Academic Editors: Ionela Andreea Neacsu and Alexandru Mihai Grumezescu

Received: 4 May 2022

Accepted: 7 June 2022

Published: 9 June 2022

Publisher's Note: MDPI stays neutral with regard to jurisdictional claims in published maps and institutional affiliations.



Copyright: © 2022 by the authors. Licensee MDPI, Basel, Switzerland. This article is an open access article distributed under the terms and conditions of the Creative Commons Attribution (CC BY) license (<https://creativecommons.org/licenses/by/4.0/>).

1. Introduction

The increasing uptake of renewables and consumer preferences for sustainability are dominating many sectors, driving a corresponding need to incorporate these aspects into new materials, product design and in-service expectations. The decarbonization of materials and products—the reduction of greenhouse gas emissions and fossil resources used in their production—carbon storage and end of life [1,2] are examples of these expectations, which are also emerging in the building and construction sector [3]. Such expectations sit alongside the impacts of products on interior living environments and requirements to use sustainable, non-formaldehyde systems for engineered wood products [4,5]. While nascent in uptake, renewable polyesters such as polylactic acid and polyhydroxy alkanate biopolymers find applications in plastics processing and also offer potential as bonding agents for wood and natural fibers [6,7]. These bio-derived plastics can already substitute fossil-fuel-based plastics, e.g., polyolefins, in packaging and consumer products [1], and it can be expected this will extend into wood panel laminates and overlays [8] and composites [9,10]. However, to better understand the potential for polyester and PLA bonding and performance characteristics in wood composites, simple qualitative and quantitative techniques are required to characterize the wood adhesion developed within these materials [7,11,12].

Reported in this study is the further development of a rapid assessment technique employing Fourier Transform Infrared (FTIR) to analyze PLA bonding of wood. This analysis methodology uses chemical spatial imaging to directly determine PLA–wood bonding at the adhesion interface of PLA–wood laminates. Chemical spatial imaging is an emerging assessment tool in wood products which has been initially employed to characterize chemical changes in modified woods [13,14] and, recently, wood adhesion [15]. With an anticipated wider applicability and uptake of this FTIR-based analysis technique, it is an appropriate time to establish protocols and quantitative metrics for how chemical spatial imaging may be applied to determine the performance of wood laminates and composites.

Based on an initial methodology using FTIR microscopy developed to characterize the PLA/wood interface [15], the chemical spatial imaging methodology is further developed using a range of PLA-bonded softwood veneer laminates to understand the adhesion bond development at the PLA–wood interface. The wood veneer panels have been prepared with differing manufacturing parameters and PLA grades to relate FTIR microscopy metrics to their interior- and wet-area performance and develop PLA adhesive performance relationships, wood composite strength and performance in dry and wet states, which have corroborated chemical spatial imaging of PLA bondline thickness and ingress into the wood substrate. These performance relationships have identified protocols and parameters for composite design and manufacture, and how PLA polymer may be employed to bond wood-composite materials. In developing performance correlations, FTIR-based spatial chemical imaging may more broadly assess the processing and performance criteria for other polyester- and polyamide-based wood composites and products.

2. Methods and Materials

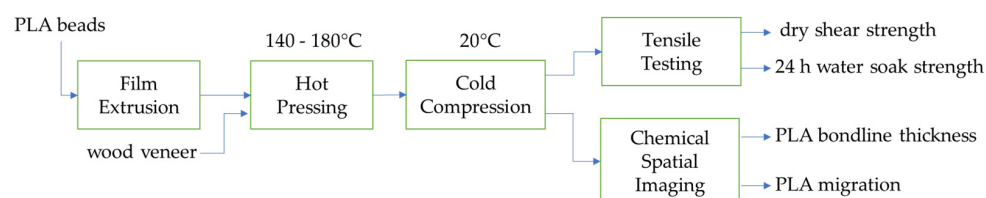
The wood veneer was commercially prepared radiata pine (*Pinus radiata* D. Don) veneer ca. 3 mm. This was cut into sheets with dimensions of 400 mm × 400 mm and equilibrated by conditioning at a temperature of 20 °C and 30% relative humidity (RH).

2.1. Poly(lactic Acid) Foil Preparation

Two poly(lactic acid) PLA polymer grades used were a semi-crystalline (3052D) PLA and amorphous (4060D) PLA obtained from Natureworks LLC (Blair, Nebraska, USA). For each PLA grade, foils were first prepared employing film extrusion. Poly(lactic acid) beads were first vacuum dried (40 °C, 16 h) before processing at 200 °C in a laboratory extruder. A 0.3 mm foil was produced as an extruded film by calendaring. Prior to panel manufacture, PLA foils were cut to the required dimensions (e.g., 200 × 400 mm strips) prior to assembling PLA veneer laminates.

2.2. PLA Laminated Veneer Panel Preparation

In this study, 5- and 7-ply PLA-radiata pine veneer laminates were prepared using a Siempelkamp laboratory press and three different platen temperatures of 140 °C, 160 °C, and 180 °C (Scheme 1).



Scheme 1. Preparation of 5-ply and 7-ply panels formed at differing pressing temperatures (140 °C, 160 °C and 180 °C) with semi-crystalline or amorphous PLA films.

For 5-ply (ca. 16 mm) panels, and as a general procedure, laminate assemblies were prepared with veneer (200 mm × 400 mm) and amorphous or semi-crystalline PLA foils by interweaving these foils between veneer laminae. The PLA foils (0.3 mm) provided a

calculated PLA application rate of ca. 265 g/m². The employed press schedule included, pressing to stops at the stated platen temperature (140 °C, 160 °C or 180 °C) and a maximum load of 45 kN. The pressed sample laminates were removed from the press and cooled to ambient temperature, maintaining a modest (5 kN) compression. The total hot-pressing and cooling times for each panel assembly and combination are provided in Table 1.

Table 1. Nominal hot-pressing and cooling times for radiata pine 5-ply laminate assemblies produced at different pressing temperatures.

Pressing Temperature °C	Hot-Pressing Time S	Cooling Time S
140	740	800
160	920	950
180	725	1020

Note: cooling times were the same across all panel sets at the stated temperature.

For 7-ply panels (300 mm × 400 mm), their manufacture followed the above general procedure to prepare and consolidate laminate assemblies. The panels were prepared at 160 °C for amorphous PLA or 180 °C for the semi-crystalline PLA grade.

In all cases, consolidated panels were trimmed to size to remove any PLA squeeze out and then stored at 23 °C and 50% RH to equilibrate for at least 5 days.

During panel consolidation, the internal panel (core) temperature profile was obtained for panel sets at each pressing temperature. A thermocouple was inserted into the core, inner bondline of each laminate assembly at the central point of the panel. After pressing was initiated, the temperature development was monitored until the core bondline temperature equilibrated to the platen temperature or the maximum pressing time achieved (Table 1).

2.3. Spatial Chemical Imaging

Representative sample specimens were recovered from the center sections of 5-ply laminated panels. Specimens were further cut into small subsections (20 mm × 20 mm) for microtoming. Specimen surfaces were first wetted with ethanol and the softened area was then smoothed by microtoming for microscopy preparation. Subsequently, the samples were dried under vacuum for at least 24 h before FTIR analysis. A Bruker Hyperion 3000 FTIR microscope was used to analyze the samples. For each specimen, at least two imaged areas (ca. 2 mm × 2 mm) of either an inner or outer bondline were used. After obtaining a low-resolution light microscopy image of the bondline region, we acquired a range of user-defined, single-point FTIR measurements across each bondline using a mercury-cadmium-telluride (MCT) detector in attenuated total reflection (ATR) mode. A resolution of 4 cm⁻¹ was used with an acquisition of 32 scans. Depending on bondline thickness, 6–8 point spectra were typically taken across a ca. 700 μm section of each imaged bondline.

Employing the OPUS 8 software (Bruker, Germany), the distinctive PLA carbonyl peak (1750 cm⁻¹) was used to develop contour plots from the FTIR point spectra [15]. These plots were projected onto the imaged cross-sections to guide the subsequent user-defined measurements of the PLA bondline thickness and PLA migration. The average penetration values were calculated from these bondline thickness and migration measurements (Equation (1)):

$$\text{Average penetration} = (\text{migration} - \text{thickness})/2 \quad (1)$$

where migration is the extent of the PLA peak projection (contour) across the bondline thickness is the PLA bondline thickness between the surfaces of veneers.

2.4. Tensile Performance Testing

Tensile testing was conducted according to ASTM D906—98(2017) and EN314-1(2014) Standards criteria. After initial conditioning, test specimens (25 mm × 100 mm) were cut from equilibrated panel samples. These specimens were then additionally cross-cut for testing individual bondlines (Supplementary Materials). For 5-ply laminates, tested bondlines were labeled either as the outer surface, or inner core bondlines. For 7-ply laminates, the bondlines were similarly identified and tested as outer (surface) or core, inner bondlines, with the middle bondlines remaining untested. Prior to testing, test specimens were further equilibrated at 23 °C and 50% RH for at least 72 h.

Shear-strength testing was conducted on an Instron 5566 universal test machine operated in tensile mode and equipped with an Instron Advanced Video Extensometer (AVE2). A preload (1 N) was applied at 0.5 mm/min and pneumatic grip pressures of 0.2 MPa used for both dry- and water-soaked test specimens. Testing speeds of 5 mm/min (up to 0.4% strain) and 50 mm/min were used and the stress at break (failing load) and the calculated tensile modulus (stiffness) were recorded. As per the standard, at least 5 specimens were tested per bondline for each sample combination of pressing temperature, pressing time and PLA grade (Table 2). The average bondline wood failures of the tested specimens were determined using visual and microscopy assessments. Specimen wood failure values were averaged and reported for each sample bondline.

Table 2. Summary of PLA bondline thickness and polymer migration and penetration results in panels formed with radiata pine veneer and semi-crystalline and amorphous PLA grades at differing pressing temperatures and times.

Panel Pressing			Inner Bondlines					Outer Bondlines				
PLA	Temp., °C	Time, S	Bondline Thickness, µm		Migration, µm		Penetration, µm	Bondline Thickness, µm		Migration, µm		Penetration, µm
			Av.	Stdev	Av.	Stdev		Av.	Stdev	Av.	Stdev	
4060D	140	600	65	16	153	29	44	90	23	211	48	61
		780	88	17	179	67	45	56	10	171	8	57
	160	920	64	11	143	44	40	82	12	179	7	48
		480	137	26	210	57	36	73	31	173	42	50
3052D	160	600	343	53	393	-	25	336	21	411	17	38
		850	269	27	321	11	26	155	21	279	62	62
	180	480	238	29	336	37	49	207	24	349	47	71

Av.: Average; St. Dev.: Standard deviation.

For cold-water soaking, test specimens were first immersed in water (20 °C) for 24 h. Before testing, specimens were recovered from the water and blotted with paper to remove excess water. Tensile testing was then conducted in their wet state using the above procedure.

3. Results and Discussion

Poly(lactic acid)-bonded laminated panels varying in panel thickness were produced with radiata pine veneer using both amorphous (4060D) and semi-crystalline (3052D) PLA grades (Table 2, Scheme 1). In producing these laminates, a range of pressing times was used, employing press temperatures of 140 °C, 160 °C and 180 °C, which have been previously shown to produce satisfactory PLA–wood adhesion [7,8,12]. These pressing regimes and PLA-veneer combinations produced a range of internal panel core temperature profiles and maximum PLA bondline temperatures during panel consolidation (Figure 1). A range of pressing times was selected from these internal temperature profiles to develop relationships between pressing temperature and time with panel performance and PLA–wood interfacial behaviors.

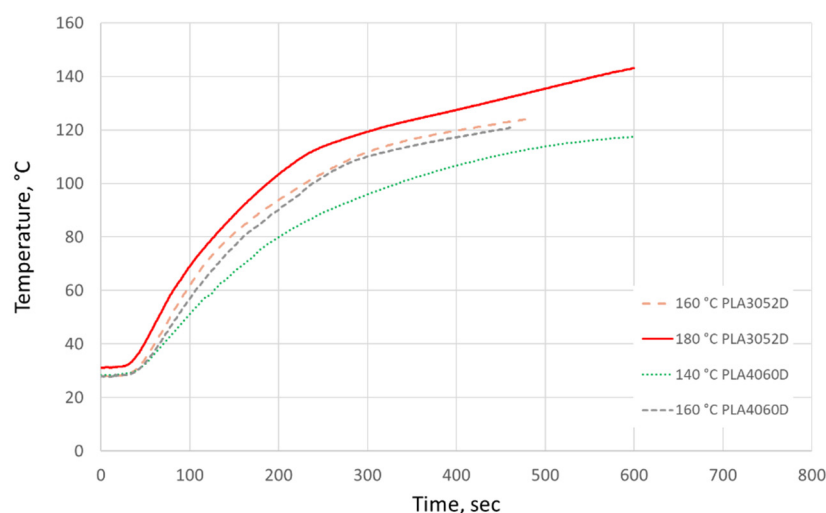


Figure 1. Selected internal panel temperature profiles for 5-ply panels formed at differing pressing temperatures (140 °C, 160 °C and 180 °C) with either semi-crystalline (3052D, purple and red) and amorphous (4060D, blue and green) PLA.

3.1. PLA–Wood Adhesion Interface Using Chemical Spatial Imaging

A comprehensive analysis of the adhesion interface developed across PLA-laminate bondlines was undertaken using FTIR microscopy. This analysis evaluated both the inner, core and outer, surface PLA bondlines of the 5-ply laminate panel sets. Building on a chemical spatial imaging methodology initially used for polyester bonding of hardwood [15], the polyester carbonyl group ($\nu\text{C}=\text{O}$, ca. 1750 cm^{-1}) of PLA was used to evaluate the distribution of PLA across the PLA–wood adhesion interface (Figure 2). This included metrics for the PLA bondline thickness and the extent of the PLA interphase developed within the wood matrix. Shown in Figure 2 is the chemical spatial imaging of a typical PLA bondline produced in this study. Evident in this image are FTIR point spectra and a PLA concentration contour plot (1750 cm^{-1} peak) across the imaged PLA bondline section. From this chemical spatial imaging, the thickness of each PLA bondline can be readily determined from both the light microscopy image as well as the PLA concentration profile evident from the PLA ester peak contour plot. Similarly, using these contour plots, the extent of PLA ingress or penetration into the wood veneer can be calculated to define the extent the PLA migration away from the bondline into the wood ultrastructure during pressing [15].

For 5-ply laminated panels formed with semi-crystalline PLA, generally, chemical spatial imaging found these panels to have greater PLA bondline thickness values than those panel sets prepared with amorphous PLA (Table 2). There were also distinctions in bondline thicknesses between outer surface and inner core PLA bondlines within panel sets and the pressing regime employed. In considering pressing temperature, 3052D inner bondlines were thicker on pressing at 160 °C ($340\text{ }\mu\text{m}$, 600 s) than at higher temperatures ($240\text{ }\mu\text{m}$, 180 °C, 480 s). This variation in bondline thicknesses has previously been observed within other PLA laminate panel products using microscopy analysis [7,12,15]. However, in this study, the pressing time at 160 °C was also important. Thinner 3052D inner bondlines were achieved at 850 s ($270\text{ }\mu\text{m}$) than a shorter pressing time (600 s). Moreover, this bondline thickness at the longer 160 °C pressing time was comparable to that achieved at 180 °C and 480 s ($240\text{ }\mu\text{m}$). Similarly, for outer bondlines formed with 3052D, analysis revealed bondlines were statistically similar on pressing for the longer pressing time at 160 °C ($155\text{ }\mu\text{m}$, 850 s) or at 180 °C ($210\text{ }\mu\text{m}$, 480 s). The shorter pressing time at 160 °C (600 s) produced a thicker outer bondline ($340\text{ }\mu\text{m}$) similar to the inner bondline and initial PLA foil thickness. Overall, semi-crystalline PLA produced panels with outer and inner bondlines, which reduce in thickness, employing either longer press times or a higher temperature.

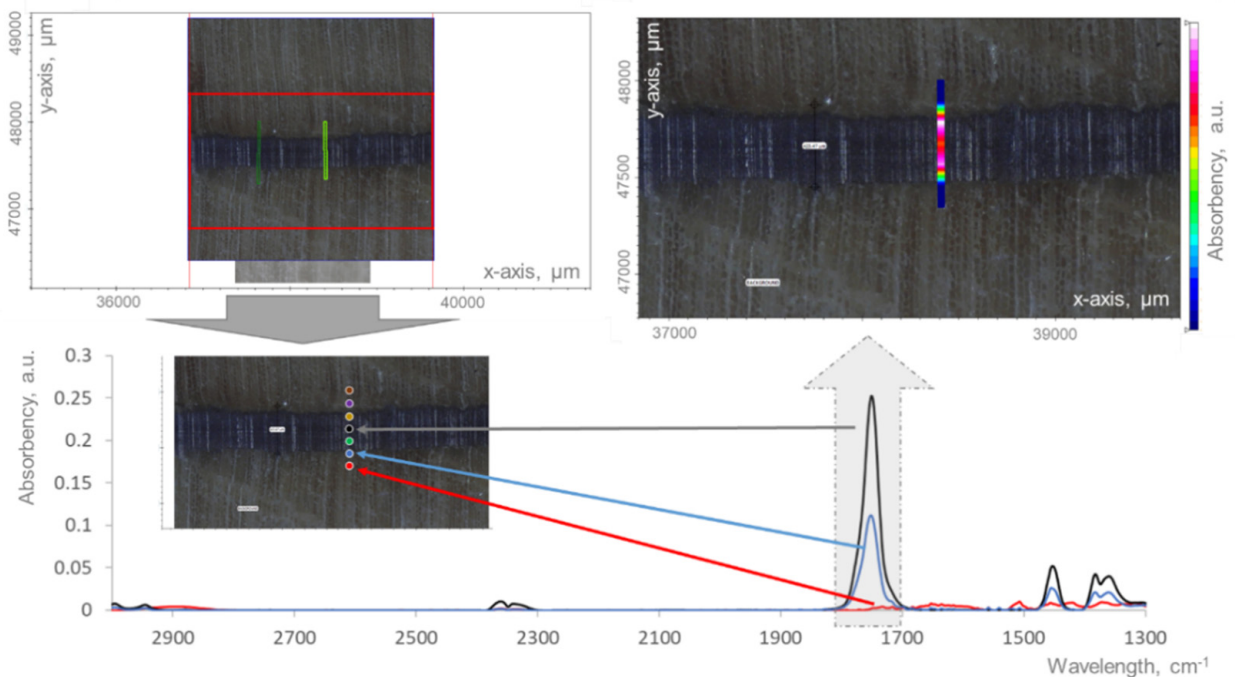


Figure 2. Chemical spatial imaging of the PLA carbonyl peak profile of the 5-ply panel outer bondline of the 160 °C, 600 s semi-crystalline sample.

An assessment of panels formed with amorphous PLA (4060D) revealed all bondlines to have lower thickness values than those formed with 3052D (Table 2). The 4060D bondline thickness values ranged between 60 and 120 μm across the differing pressing temperatures and times employed. At 140 °C, the outer bondline thickness (90 μm) was similar on pressing for 600 or 780 s. A similar outer bondline thickness was found at 160 °C, including using an extended pressing time of 920 s. For 4020D inner bondlines, measurements show these were comparable to outer bondline thickness values. For panels formed at 160 °C, there was a significant reduction in inner bondline thickness at an extended pressing time (60 μm , 920 s), a trend similarly observed for semi-crystalline PLA using a long pressing time (160 °C, 850 s). Moreover, with these 4060D lower bondline thickness values, it was evident the local surface roughness of veneers was impacting bondline measurements with greater variability observed between sample replicates.

From chemical spatial imaging assessments of PLA carbonyl peak (1750 cm^{-1}) concentration profiles, analysis revealed PLA migration (penetration) away from the bondline into the wood ultrastructure was more dependent on the pressing temperature and time than the PLA grade (Table 2). Calculated PLA penetration values from PLA concentration projections of bondline cross-sections revealed PLA migration values ranged from 20 to 80 μm . With semi-crystalline PLA, PLA migration was generally greater in outer bondlines, with average penetration values of 40 to 70 μm compared to <50 μm for inner bondlines. At 160 °C, outer bondline migration increased from 40 μm (600 s) to 60 μm at the longest pressing time (850 s), with 70 μm penetration achieved on pressing at 180 °C (480 s). For 3052D inner bondlines, PLA penetration values of just 25 μm were achieved at 160 °C, with this extending to 50 μm at the highest pressing-temperature.

For amorphous PLA, the rates of PLA penetration were not distinguished by the position of bondlines within panels. Chemical spatial imaging determined 4060D PLA migration from outer bondlines (50–60 μm) was greater than inner bondlines (ca. 40 μm). Moreover, there was little distinction in average penetration values for panels formed at either 140 °C or 160 °C. This was consistent with the PLA polymer properties and flow of this PLA type in contrast with the higher melt of the semi-crystalline PLA [7]. Overall, while distinctions in penetration values were evident across the wider panel series, collectively, the PLA migration from the bondline was considered 1–2 wood-cells deep, with this

visually evident in spatial chemical images (Supplementary Materials) and consistent with previous qualitative assessments with other visualization techniques [7,8]. Moreover, this imaging corroborated the assessments with PLA concentration profiles decreasing sharply away from the bondline (Figure 3), with this qualitative assessment relatively uniform across the samples evaluated.

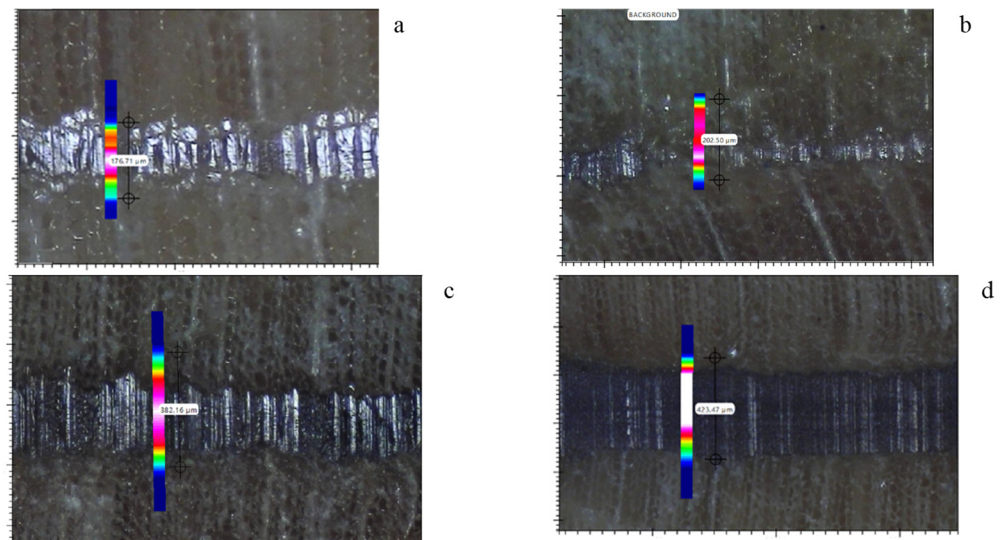


Figure 3. Selected examples from chemical spatial imaging analysis which show PLA bondline thickness to vary substantially, ranging from 60 mm and 340 mm across the 5-ply panel sets ((a): 140 °C, 600 s, outer bondline 176.71 µm; (b): 160 °C, 480 s, outer bondline 202.50 µm; (c): 180 °C, 480 s, outer bondline 382.16 µm; (d): 160 °C, 600 s, outer bondline 423.47 µm).

Employing chemical spatial imaging revealed softwood-PLA bondline thickness and PLA migration away from bondlines could be readily quantified via FTIR peak contour analysis. Poly(lactic acid) bondline thickness and penetration values could be related to the PLA mobility and migration at temperatures achieved by the pressing regime and, in some cases, further distinguished by the bondline position in the laminated panel (Table 2). The internal temperatures achieved on panel consolidation will contribute to the melt viscosity and flow of the PLA polymer (Figure 1, and Supplementary Materials) [16]. The potential for PLA to flow and ingress into the wood ultrastructure greatly increases as the viscosity is significantly reduced at higher temperatures. This was particularly evident for semi-crystalline PLA, where 5-ply panel internal temperatures exceeded the PLA melt (ca. 140 °C) more rapidly at 180 °C than 160 °C platen temperature. A comparison of bondline thicknesses shows values decreased for pressing times >600 s at 160 °C and >480 s at higher temperatures (Table 2). This corresponded to internal panel temperatures exceeding 140 °C during pressing 3052D laminates (Figure 1). For 7-ply 3052D panels, internal temperatures of 140 °C were achieved in 480 s, which was also suggested by their performance testing (Figure 2, Tables 2 and 3). For amorphous PLA panels, the melt flow of this PLA grade is at a lower temperature [17] as indicated by the similar bondline thickness values across the 140 °C and 160 °C pressing regimes employed. Internal panel temperatures of 120 °C can be achieved with 140 °C platen temperatures after 480 s and ca. 300 s on pressing at 160 °C (Figure 1). In comparison, industrially, softwood veneer laminates are typically pressed below 160 °C to achieve core temperatures <110 °C.

Table 3. Summary of tensile testing results of 5-ply and 7-ply panels formed with radiata pine veneer and semi-crystalline and amorphous PLA grades at differing pressing temperatures and times before soaking.

Polymer	Press Temp, °C	Press Time, S		Inner Bond Dry.				Outer Bond Dry.			
				Tensile Strength, MPa		Wood Failure, %		Tensile Strength, MPa		Wood Failure, %	
				Av.	Std Dev	Av.	Std Dev	Av.	Std Dev	Av.	Std Dev
4060D	140	780	5-ply	2.81	0.18	94	9	2.84	0.21	96	5
	140	600	5-ply	4.26	0.67	85	20	3.10	0.58	74	21
	160	920	5-ply	4.15	0.72	95	9	4.63	0.86	92	8
	160	600	5-ply	3.90	0.37	77	15	4.32	1.30	83	10
	160	480	5-ply	3.89	0.27	84	9	4.17	0.49	92	8
3052D	160	850	5-ply	5.66	1.39	95	5	5.75	0.99	88	16
	160	600	5-ply	2.24	0.59	30	0	1.80	0.50	20	12
	180	920	5-ply	5.30	1.53	66	31	4.86	0.68	63	32
	180	600	5-ply	3.24	1.07	68	15	2.82	0.57	52	34
	180	480	5-ply	3.79	0.48	92	6	4.62	0.99	78	22
4060D	180	360	5-ply	2.21	0.27	50	12	1.61	0.29	4	5
	160	600	7-ply	4.23	0.28	74	9	4.43	0.49	90	14
3052D	160	480	7-ply	5.56	0.75	90	10	4.58	0.36	98	4
	180	480	7-ply	2.15	0.48	26	9	3.47	0.45	38	19
	180	360	7-ply	2.88	0.37	38	18	2.95	0.56	14	5

Av.: Average; St. Dev.: Standard deviation.

Furthermore, while bondline thickness values ranged between 60 μ m and 340 μ m across the sample series, the difference in calculated PLA penetration values was reduced. Penetration values were 25 μ m to 70 μ m representative of PLA migration 1 to 2 wood cells deep from the bondline. These PLA values from chemical spatial imaging were consistent with observations of other PLA-softwood bondlines and reported penetration rates of other hydrophobic linear polymer adhesive and paraffin wax systems [18]. Moreover, in this study, not insignificant quantities of PLA “squeeze out” were observed for some laboratory panels, which may explain discrepancies in bondline thickness and extent of PLA migration and penetration values for some samples, as well as opportunities for application rate and processing improvements.

3.2. Bond Strength Development and Performance

Tables 3 and 4 show tensile testing results evaluating individual bondlines from 3-, 5- and 7-ply laminated samples. This testing was undertaken with samples either dry (Table 3), or after 24 h cold-water soaking (Table 4). For 5-ply samples prepared with amorphous PLA, these were found to have greater dry strength when pressed at 160 °C than those prepared at 140 °C. Generally, these 4060D samples were not distinguished by their pressing times when pressing at 160 °C. Similar tensile strength values (ca. 4 MPa) were apparent for both outer and inner bondlines at 160 °C, which was comparable across pressing times from 480 to 920 s. In contrast with 4020D, laminated 5-ply samples prepared with semi-crystalline PLA were distinguished by their pressing temperature and pressing time. For 3052D samples pressed at 160 °C, significantly greater bond strength was developed only after pressing for an extended time. Generally, samples pressed for \leq 600 s had strength values of ca. 2 MPa, with this increasing to $>$ 5.5 MPa at the longest press time (850 s). Interestingly, in previous work, lower bond-strengths had been similarly observed with

semi-crystalline PLA and softwood combinations [8]. However, at 180 °C, relatively high bond strength values were developed at 480 s for 3052D samples, comparable to longer press times (920 s). Tensile testing also revealed no distinctions in performance between outer and inner bondlines of these 180 °C 3052D samples. Lastly, it is noteworthy that tensile testing exhibited high variability within some sample replicates (Table 3). This variability is attributed to both the relatively higher strength values (>4 MPa) exhibited by PLA-bonded samples and associated high rates of wood failure (>75%) together with the potential degradation of the wood substrate introduced by the extended pressing regimes employed in this study.

Table 4. Summary of tensile testing results after 24 h water soaking for 5- and 7-ply panels formed with radiata pine veneer and semi-crystalline and amorphous PLA grades at differing pressing temperatures and times.

Polymer	Press Temp, °C	Press Time, S	Inner Bond Wet.				Outer Bond Wet.				
			Tensile Strength, MPa		Wood Failure, %		Tensile Strength, MPa		Wood Failure, %		
			Av.	Std Dev	Av.	Std Dev	Av.	Std Dev	Av.	Std Dev	
4060D	140	780	5-ply	2.57	0.15	87	16	3.46	0.23	95	9
	140	600	5-ply	1.50	0.83	59	27	2.38	0.49	80	16
	160	480	5-ply	3.08	0.17	90	17	2.87	0.17	96	5
	160	600	5-ply	2.76	0.10	96	5	3.22	0.37	100	0
	160	920	5-ply	2.89	0.21	93	8	2.45	0.37	74	9
	160	850	5-ply	2.37	0.20	82	11	2.28	0.82	74	21
3052D	160	600	5-ply	1.13	0.25	60	12	0.38	0.27	23	6
	180	920	5-ply	4.54	0.65	52	13	3.89	0.36	68	18
	180	600	5-ply	1.70	0.67	43	40	0.46	N/A	10	N/A
	180	480	5-ply	1.94	0.34	70	20	2.04	0.66	36	5
	180	360	5-ply	1.49	0.14	58	32	2.01	N/A	95	N/A

Av.—Average; St. Dev.—standard deviation.

For 7-ply samples, tensile testing revealed high-strength values in panels bonded with amorphous PLA, whereas lower bondline strength was evident in panels formed with semi-crystalline PLA. For 4060D samples produced with a 160 °C press temperature, bondlines were found to have strength values of ca. 4.5 MPa, which were comparable to those of the 5-ply laminated panels. Testing also revealed no distinctions between the outer and inner, core bondlines of panels produced at differing pressing times at this temperature. The combination of 3052D PLA and a 180 °C press temperature produced bondlines with tensile strength values ranging between 2 and 4 MPa. At the shorter pressing time, the bond strength of outer and inner bondlines was comparable (ca. 3 MPa). A longer pressing time produced outer bondline strength (ca. 4 MPa) similar to the 4060D samples, but inner bondlines were significantly lower in strength (ca. 2 MPa). The tensile strength values for these inner bondlines did not significantly differ to those produced at the shorter pressing time.

Wet-strength tensile testing was undertaken to further establish performance variations between PLA grades and panel-pressing regimes (Table 3). Previously, wet-strength performance evaluations have been a better indicator of PLA-hardwood bondline strength development than testing samples dry [8]. This was similarly the case in this study. For the amorphous PLA, 24 h cold-water soaking revealed 4060D samples required longer pressing time (780 s) at 140 °C to achieve wet-strength bondline performance values of ca. 3 MPa. At 160 °C, this wet-strength performance of 4060D samples was achieved at

480 s with no distinction in performance at longer pressing time. At this higher pressing temperature, the wet strength of inner bondlines was similar and did not exhibit the high variability observed in dry testing. In the case of semi-crystalline PLA bondlines, wet-strength testing revealed the performance of 3052D 5-ply samples was sensitive to the pressing temperature employed. As found for dry-strength testing, a longer press time was required to develop bondline wet strength at 160 °C. Only at the longest pressing time (850 s) did 160 °C samples achieve a wet-strength value >2 MPa. However, pressing at 180 °C produced a comparable wet-strength performance on pressing for 360 or 480 s. The greatest wet-strength performance (ca. 4 MPa) in this study was achieved with 3052D PLA and an extended pressing time (920 s), producing a wet-strength value comparable to that established in dry-strength testing.

For 7-ply laminates, water-soak testing also revealed lower wet-strength performance for samples produced with shorter pressing regimes. With the amorphous PLA, pressing at 160 °C for 400 s produced a performance of <3 MPa after water soaking, a wet-strength value comparable to 5-ply 4060D samples prepared at 140 °C and 600 s. Nonetheless, a longer pressing time (600 s) produced wet-strength values of ca. 4 MPa. In the case of the semi-crystalline PLA, pressing at 180 °C led to wet-strength values of ca. 2 MPa. As above, this tensile strength value on water soaking was similar to most 5-ply panels formed with semi-crystalline PLA.

In relating the performances of PLA-bonded laminate panels, generally, the pressing regime, the PLA grade and the PLA mobility at the adhesion interface determined the PLA bonding efficacy (Table 3). Trends are also evident for PLA laminates formed from hardwoods [8]. For the amorphous PLA, greater tensile strength was achieved at 160 °C (ca. 4 MPa) than at 140 °C (ca. 3 MPa) and, except for a short pressing time (160 °C, 480 s), relatively uniform, thin bondlines (60 µm–90 µm) were produced at these temperatures. In all cases, calculated penetration values ranged between 40 µm and 60 µm, with outer bondlines associated with greater PLA penetration. While no relationship was evident between dry tensile strength and bondline thickness values ($R^2 < 0.1$), there was a correlation ($R^2 = 0.86$) with PLA penetration values (50–60 µm) for outer bondlines (Supplementary Materials). This outcome was not unsurprising, as all samples formed with amorphous PLA achieved comparable dry tensile-strength values. Similarly, as most 4060D samples also exhibit comparable cold-water-soak performance (2.5 MPa–3.0 MPa) across the differing pressing regimes, only the outer bondline thickness could be correlated ($R^2 = 0.96$) with cold-water-soak performance. For panels bonded with semi-crystalline PLA, these had a greater range of dry and wet tensile-strength values (1 MPa–5 MPa), together with PLA thickness and penetration values of 155 µm to 340 µm and 25 µm to 70 µm, respectively. Dry tensile-strength values could be correlated with both inner and outer bondline thicknesses and outer bondline penetration values. Moreover, in this study, the greatest correlation between panel performance and the PLA adhesion interface was with 3052D wet-strength values. There was an excellent correlation between wet-strength performance and outer bondline thickness ($R^2 = 0.97$) and penetration ($R^2 = 0.86$) values. For inner bondlines, thickness and penetration values could also be related to sample tensile strength values ($R^2 < 0.6$) after water soaking with panel internal temperature development, likely contributing to the variability of the latter (Figure 1).

Overall, satisfactory PLA–wood bonding was achieved by pressing panels at higher temperature or for longer pressing times. With amorphous PLA, this panel performance was achieved at a lower temperature or a reduced pressing time, which is more typical of conventional plywood manufacture. In each case, the higher tensile strength values and wood failure rates were achieved with internal panel temperatures sufficient to melt and promote PLA migration into the wood ultrastructure to reinforce bondlines (Table 2).

4. Conclusions

The application of chemical spatial imaging can readily determine the interfacial adhesion developed between PLA polyester and wood. Both the bondline thickness and extent

of PLA migration from the bondline into the wood matrix can provide quantifiable information regarding the impacts of panel-processing parameters. Higher pressing temperatures and longer pressing times were generally associated with greater PLA ingress into the wood and thinner PLA bondlines. This was particularly evident for the semi-crystalline PLA and, to a lesser extent, for amorphous PLA. Moreover, the impact of internal panel temperatures achieved on pressing was also key to further distinguishing PLA mobility and migration between panel outer and core bondlines.

In this study, the combination of chemical spatial imaging with performance testing of individual panel bondlines was crucial to understanding PLA-laminated panel performance. For the first time, the impacts of pressing regimes and resulting internal panel temperature profiles have been related to the performance of PLA grades and laminated panel mechanical performance in both the dry and wet state. Thinner PLA bondlines were associated with greater dry-strength, which was readily achieved with both amorphous and semi-crystalline PLA grades. This was consistent with earlier findings of our more extensive study, and indicative of PLA migration into wood ultrastructure and reinforcement of the bondline. While dry testing established distinctions in PLA–wood adhesion interface due to pressing temperature, 24 h water soaking determined satisfactory adhesive wet-strength performance could be maintained with semi-crystalline PLA in combination with higher-temperature (180 °C) pressing regimes. Analysis revealed panel bond-strength was developed with low rates of PLA penetration into the wood veneer, but maximum strength values were attained with greater PLA penetration. Moreover, the combination of greater temperature and pressing time with semi-crystalline PLA was required for panel bondlines to maintain comparable wet performance after 24 h water soaking. To achieve this 5- and 7-ply performance, pressing for 10–20 min may be unrealistic, but a mixed use of PLA crystallinity grades may be considered for commercial production PLA bonded panels. Practically, at larger scales, it is expected that processing PLA with wood veneers will need to balance processing times with commercial expectations, but the combination of a 100% sustainable bonding agent and no added formaldehyde system will be attractive to building and construction materials.

Supplementary Materials: The following are available online at <https://www.mdpi.com/article/10.3390/fib10060051/s1>. Figure S1: Cutting pattern employed to generate 25 mm × 100 mm test specimens which were then cross-cut to isolate the bondline (inner and outer) for testing bond line; Figure S2: Selected example from chemical spatial imaging analysis showing extent of PLA migration (penetration) from the bondline. Semi-crystalline PLA, 180 °C, 360 s; Figure S3: Selected internal panel temperature profiles for 5-ply panels formed at 160 °C (top) and 180 °C (bottom) pressing temperatures with ether semi-crystalline PLA (3052D); Figure S4: Comparisons of PLA bondline thickness and penetration values (5-ply samples); Figure S5: Comparisons of bondline tensile strength values (5-ply samples); Figure S6: Comparisons of bondline tensile strength values (5-ply samples); Figure S7: Comparisons of bondline tensile strength values (7-ply samples); Table S1: Relationships of dry and wet tensile strength with PLA bondline thickness and penetration values for inner and outer bondlines of 5-ply panels; Table S2: Summary of tensile testing results of 5-ply panels formed with radiata pine veneer and semi-crystalline and amorphous PLA grades at differing pressing temperatures and times before soaking.

Author Contributions: Conceptualization, W.J.G. and M.G.; formal analysis, W.J.G., D.T. and M.G.; investigation, supervision, W.J.G. and M.G.; project administration W.J.G. and M.G.; writing—original draft preparation, W.J.G.; writing—review W.J.G., M.G. All authors have read and agreed to the published version of the manuscript.

Funding: This research received no external funding.

Institutional Review Board Statement: Not applicable.

Informed Consent Statement: Not applicable.

Data Availability Statement: Not applicable.

Acknowledgments: The authors are grateful for the resourcing provided by Scion. D.T. was a recipient of a Toi Ohomai Institute of Technology summer internship and placement supported by Scion.

Conflicts of Interest: The authors declare no conflict of interest. The funders had no role in the design of the study; in the collection, analyses, or interpretation of data; in the writing of the manuscript; or in the decision to publish the results.

References

1. Bishop, G.; Styles, D.; Lens, P.N.L. Environmental performance comparison of bioplastics and petrochemical plastics: A review of life cycle assessment (LCA) methodological decisions. *Resour. Conserv. Recycl.* **2021**, *168*, 105451.
2. Nagarajan, V.; Mohanty, A.K.; Misra, M. Perspective on Polylactic Acid (PLA) based Sustainable Materials for Durable Applications: Focus on Toughness and Heat Resistance. *ACS Sustain. Chem. Eng.* **2016**, *4*, 2899–2916. [[CrossRef](#)]
3. Arehart, J.H.; Hart, J.; Pomponi, F.; D'Amico, B. Carbon sequestration and storage in the built environment. *Sustain. Prod. Consum.* **2021**, *27*, 1047–1063. [[CrossRef](#)]
4. Gonçalves, D.; Bordado, J.M.; Marques, A.C.; Galhano dos Santos, R. Non-Formaldehyde, Bio-Based Adhesives for Use in Wood-Based Panel Manufacturing Industry—A Review. *Polymers* **2021**, *13*, 4086.
5. Solt, P.; Konnerth, J.; Gindl-Altmutter, W.; Kantner, W.; Moser, J.; Mitter, R.; van Herwijnen, H.W. Technological performance of formaldehyde-free adhesive alternatives for particleboard industry. *Int. J. Adhes. Adhes.* **2019**, *94*, 99–131. [[CrossRef](#)]
6. Bakken, A.C.; Taleyarkhan, R.P. Plywood wood based composites using crystalline/amorphous PLA polymer adhesives. *Int. J. Adhes. Adhes.* **2020**, *99*, 102581. [[CrossRef](#)]
7. Luedtke, J.; Gaugler, M.; Grigsby, W.J.; Krause, A. Understanding the development of interfacial bonding within PLA/wood-based thermoplastic sandwich composites. *Ind. Crops Prod.* **2019**, *127*, 129–134. [[CrossRef](#)]
8. Grigsby, W.J.; Puri, A.; Gaugler, M.; Lüedtke, J.; Krause, A. Bonding Wood Veneer with Biobased Poly(Lactic Acid) Thermoplastic Polyesters: Potential Applications for Consolidated Wood Veneer and Overlay Products. *Fibers* **2020**, *8*, 50. [[CrossRef](#)]
9. Peltola, H.; Pääkkönen, E.; Jetsu, P.; Heinemann, S. Wood based PLA and PP composites: Effect of fibre type and matrix polymer on fibre morphology, dispersion and composite properties. *Compos. Part A Appl. Sci. Manuf.* **2014**, *61*, 13–22. [[CrossRef](#)]
10. Tao, Y.; Wang, H.; Li, Z.; Li, P.; Shi, S.Q. Development and application of wood flour-filled polylactic acid composite filament for 3d printing. *Materials* **2017**, *10*, 339. [[CrossRef](#)] [[PubMed](#)]
11. Gaugler, M.; Luedtke, J.; Grigsby, W.J.; Krause, A. A new methodology for rapidly assessing interfacial bonding within fibre-reinforced thermoplastic composites. *Int. J. Adhes. Adhes.* **2019**, *89*, 66–71. [[CrossRef](#)]
12. Grigsby, W.; Gager, V.; Recabar, K.; Krause, A.; Gaugler, M.; Luedtke, J. Quantitative Assessment and Visualisation of the Wood and Poly(Lactic Acid) Interface in Sandwich Laminate Composites. *Fibers* **2019**, *7*, 15. [[CrossRef](#)]
13. Bonifazi, G.; Calienno, L.; Capobianco, G.; Monaco, A.L.; Pelosi, C.; Picchio, R.; Serranti, S. A new approach for the modelling of chestnut wood photo-degradation monitored by different spectroscopic techniques. *Environ. Sci. Pollut. Res.* **2017**, *24*, 13874–13884. [[CrossRef](#)] [[PubMed](#)]
14. Mäkelä, M.; Altgen, M.; Belt, T.; Rautkari, L. Hyperspectral imaging and chemometrics reveal wood acetylation on different spatial scales. *J. Mater. Sci.* **2021**, *56*, 5053–5066. [[CrossRef](#)]
15. Grigsby, W.J.; Torayno, D.; Gaugler, M.; Luedtke, J.; Krause, A. Chemical imaging of the polylactic acid—Wood adhesion in-terface of bonded veneer products. *Fibers* **2022**, *10*, 17. [[CrossRef](#)]
16. Garlotta, D. A literature review of poly(lactic acid). *J. Polym. Environ.* **2001**, *9*, 63–84. [[CrossRef](#)]
17. Carrasco, F.; Pagès, P.; Gámez-Pérez, J.; Santana, O.; MasPOCH, M.L. Processing of poly(lactic acid): Characterisation of chemical structure, thermal stability and mechanical properties. *Polym. Degrad. Stab.* **2010**, *95*, 116–125. [[CrossRef](#)]
18. Grigsby, W.J.; Thumm, A. Visualising the wood fibre-adhesive interface: Implications for adhesive behaviour, performance and design. In Proceedings of the International Conference on Wood Adhesives, Toronto, ON, Canada, 9–11 October 2013.